Quantitative Relationships between Soil Macropore Characteristics and Preferential Flow and Transport

Lifang Luo*

    U.S. Salinity Laboratory
Riverside, CA 92507

    and
Dep. of Environmental Sciences
University of California
Riverside, CA 92521

Henry Lin

    Dep. of Crop and Soil Sciences
116 ASI Building
The Pennsylvania State University
University Park, PA 16802

John Schmidt

    Pasture Systems & Watershed
      Management Research Unit
USDA– ARS
Building 3702 Curtin Road
University Park, PA 16802

Quantitative relationships between soil structure, especially macropore characteristics, and soil hydraulic properties are essential to improving our ability to predict flow and transport in structured soils. The objectives of this study were to quantitatively relate macropore characteristics to saturated hydraulic conductivity (K_{sat}) and dispersivity (λ) and to identify major macropore characteristics useful for estimating soil hydraulic properties under saturated condition. Large intact soil columns were taken from two land uses (cropland and pasture) of the same soil type (a Typic Hapludalf), with four replicates for each land use. The soil columns were scanned using X-ray computed tomography (CT) to obtain macropore parameters including macroporosity, length density, mean tortuosity, network density, hydraulic radius, path number, node density, and mean angle. The K_{sat} of the whole soil column, as well as each soil horizon within the column, and solute breakthrough curve (BTC) of $CaBr_2$ were determined for each column. For all eight soil columns studied, macroporosity and path number (the number of independent macropore paths between two boundaries) explained 71 to 75% of the variability in the natural logarithm of K_{sat} values of the whole soil columns as well as of individual soil horizons. The traditional convection–dispersion equation (equilibrium model) simulated the BTCs well for all soil columns except one with an earthworm hole passing through the entire column, for which the two-region model (non-equilibrium model) was required. The path number, hydraulic radius, and macropore angle were the best predictors for λ, explaining 97% of its variability. Correlation between λ of the whole soil columns and K_{sat} values of the Bt horizons (but not A horizons) implied that the dispersivity was mainly controlled by the horizon with the lowest K_{sat} in the soil columns. These results indicate that the most useful macropore parameters for predicting flow and transport under saturated condition in structured soils included macroporosity, path number, hydraulic radius, and macropore angle.

Abbreviations: 3-D, three-dimensional; BTC, breakthrough curve; CT, computed tomography; CDE, convection-dispersion equation; C, cropped Hagerstown; P, pastured Hagerstown; K_{sat}, saturated hydraulic conductivities; PTF, pedotransfer function; PVC, polyvinyl chloride; D, solute dispersion coefficient.

In recent decades, soil macropores as preferential pathways for water, air, and chemical movement through soils have received considerable attention because of their significant impacts on water quality and hydrological response (e.g., Beven and Germann, 1982; Jarvis, 2007). Soil macropores are distinctly different from fine pores in soil matrix not only in pore size but also in hydraulic functions related to different continuity, tortuosity, and connectivity (Jarvis, 2007, Luo at el., 2010). Macropore flow may dominate near-saturated flow even though macropores may only constitute a small fraction of total soil porosity (Luxmoore et al., 1990; Lin et al., 1996).

To estimate macropore flow and solute transport, hydraulic properties (e.g., hydraulic conductivity and dispersion coefficient) associated with macropores have to be accurately determined. Experimental measurements of soil hydraulic parameters are generally time-consuming and costly. Thus, various approaches have been developed in the past to estimate soil hydraulic properties from basic soil properties. These models have used particle-size distribution (Arya and Paris, 1981), pore-size distribution (van Genuchten, 1980; Kosugi, 1999), soil morphological features (Lin et al., 1999), and many other characteristics (Pachepsky and Rawls, 2004). Most models based on pore-size distribution assume a cylindrical pore shape and have not adequately considered the tortuosity, continuity, and connectivity of

pores, which have been recognized as important to soil hydraulic functions (e.g., Lin et al., 1996; Bouche and Al-Addan,1997; Perret et al., 2000; Vervoort and Cattle, 2003; Bastardie et al., 2003). The Kozeny–Carmen equation is one of the most widely applied methods for estimating saturated hydraulic conductivity (K_{sat}) based on hydraulic radius, tortuosity, and specific area. One concern is that hydraulic radius concept may be inadequate for describing structured media, such as clay soils with macropores (Hillel, 1998, p. 183–189). Therefore, considerable uncertainty and error can be involved when estimating hydraulic conductivity at near-saturated conditions in macroporous soils (Mallants et al., 1997).

The potential for non-equilibrium flow and transport in macropores has been associated with the degree of soil structure (Vervoort et al., 1999; Ersahin et al., 2002; Shaw et al., 2000; Merdun and Quisenberry, 2004), clay content (Shaw et al., 2000; Franklin et al., 2007), macropore distribution (Franklin et al., 2007), and organic matter content (Jarvis, 2007). Jarvis (2007) reviewed the factors influencing non-equilibrium flow and transport in macropores and developed a conceptual model to describe the potential for non-equilibrium flow and transport in macropores using soil structure and various factors controlling soil structure formation and degradation. He suggested that the potential for physical non-equilibrium flow and transport in macropores increases in structural pore systems with a poorly developed hierarchy, until some critical point is reached when the continuity of macropores becomes limiting. Shaw et al. (2000) found a greater degree of preferential flow with more clay content and better soil structural development. They developed pedotransfer functions (PTFs) between soil properties and model parameters for solute transport. Jarvis (2007) showed that organic matter content and geometric mean particle size could explain 60% of the variation in the mass transfer coefficient estimated from the dual-permeability model MACRO. Goncalves et al. (2001) developed PTFs to link basic soil properties to parameters of a non-equilibrium convection–dispersion equation (two-region model) using neural network and bootstrap analysis.

However, quantitative relationships between measured three dimensional (3-D) macropore characteristics (including macroporosity, size, tortuosity, continuity, inclination, connectivity, and other characteristics) and hydraulic conductivity and solute transport variables have not been fully understood in natural macroporous soils. Traditional methods have been limited in quantifying complex macropore structure. Due to the difficulty of obtaining macropore data and the complex nature of macropore geometry and topology, artificial macropores in packed soil columns have been used to study the effect of macropore characteristics on macropore flow (e.g., Köhne and Mohanty, 2005; Akay and Fox, 2007). Thin-section (Schaap and Lebron, 2001) and dye tracing (Franklin et al., 2007) are destructive and constrained for reconstructing 3-D macropore geometry. In contrast, CT is a nondestructive and powerful imaging technique for observing and quantifying macropore networks in soils (e.g., Anderson et al., 1992; Luo et al., 2008). Anderson et al. (2003) estimated K_{sat} from spatially varied porosity determined from CT images using the Kozeny formula. Perret et al. (2000) quantified macropore hydraulic radius from CT images and calculated the flux through macropores using a modified version of Poiseuille's law and Manning's equation.

The objectives of this study were to examine quantitative relationships between intact soil macropore characteristics and saturated soil column hydraulic properties (particularly K_{sat} and λ) and to identify the most important macropore features that control soil hydraulic functions under saturated condition.

MATERIALS AND METHODS
Sites and Soils Studied

The soils investigated in this study represent one of the most productive agricultural soils in Pennsylvania—the Hagerstown silt loam (fine, mixed, semiactive mesic Typic Hapludalfs). Two representative land uses, cropland and pasture, were selected to examine the effects of land use on soil structure and hydraulic properties. The cropland site had been in a rotation of 2 yr of corn (*Zea mays* L.) and 1 yr of soybean [*Glycine max (L.) Merr.*] with conventional tillage. The pasture site had been under perennial grass (predominantly orchardgrass [*Dactylis glomerata* L.]) and regularly grazed by cows (*Bos taurus*). A backhoe was used to carefully push polyvinyl chloride (PVC) pipes (102 mm in diameter and about 350 mm in length, with bottom edge sharpened) into the soil vertically in a very careful manner (see Luo et al. [2008] for further details). Five soil columns were taken from each site in July 2007. Three soil horizons were contained within each soil column collected (Table 1). Besides these larger soil columns, three small vertical intact soil cores, 55 mm in diameter and 60 mm in length, were taken from each

Table 1. Soil profile features and their basic properties. Numbers in parentheses are standard errors (*n* = 3).

Land use (symbol)	Soil horizon	Depth	Pedality (structure)†	Roots‡	Bulk density	Sand	Silt	Clay	Organic matter
		cm			g cm^{-3}		—%—		
Cropland (C)	Ap1	0–15	2 f-m sbk	3 vf-f	1.34 (0.02)	19	65	16	4.5
	Ap2	15–31	2 m pl parting to 2 m sbk	3 f	1.35 (0.03)	17	68	15	3.5
	Bt1	31–36+	2 m sbk	2 f	1.46 (0.02)	23	52	25	1.9
Pasture (P)	A1	0–15	3 f-m gr	3 vf-m	1.16 (0.01)	24	62	13	7.5
	A2	15–32	3 m sbk	3 f	1.27 (0.00)	24	59	16	3.6
	Bt1	32–36+	2 m sbk	2 f	1.37 (0.04)	18	62	21	2.0

† Pedality is described using ped grade, ped size and ped shape: 1, 2, 3 for weak, moderate, and strong ped grades, respectively; vf, f, m and c for very fine, fine, medium and coarse ped sizes, respectively; sbk, gr, and pl for subangular blocky, granular and platy ped shapes, respectively.

‡ Roots are described using the quantity and size: 1, 2, 3 for few, common and many, respectively; vf, f, m, c, and vc for very fine, fine, medium, coarse and very coarse root sizes, respectively.

horizon to measure soil bulk density and K_{sat}. Soil samples were also collected from each horizon to measure particle-size distribution using a simplified method (Kettler et al., 2001) and organic matter content using loss on ignition method (Schulte and Hopkins, 1996). Basic soil properties are summarized in Table 1.

Quantification of Three-Dimensional Macropore Networks

All soil columns were scanned using a medical CT (Universal System, Inc., Solon, OH). In-plane pixel sizes vary between 0.25 to 1 mm on a side for objects from 120 to 480 mm in diameter. Slice thickness can vary between 1 and 10 mm. The scanner uses excitation voltages from 80 to 140 kV with maximum power of about 13 kJ s^{-1}. The images produced were 512 × 512 pixels. Based on the CT images, columns with noticeable structural disturbance inside the column (e.g., unnatural sidewall pores or cracks) were not used in this study. For each land use, four soil columns were deemed intact and used for further analysis of soil hydraulic properties and solute breakthrough experiments.

Detailed procedures of image analysis and quantification of soil macropore characteristics are described in Luo et al. (2010). Only a brief summary is provided here. Figure 1 shows representative 3-D macropore networks reconstructed from the CT images. Macroporosity, macropore length density, node density, network density, path number, mean tortuosity, hydraulic radius, and mean angle of 3-D macropores were quantified for each column and each horizon contained in the eight columns using Avizo version 5 (Mercury Computer Systems, Chelmsfold, MA) and a custom developed computer program in C (Luo et al., 2010). Table 2 lists the definitions of various macropore characteristics used in this study.

Experimental Procedures for Flow and Transport Measurements

Since some soil pore space may be entrapped with air using a typical laboratory method (e.g., submerging soil sample slowly and gradually in water), we used a vacuum to improve the soil column saturation ratio (Fig. 2a) and to provide a better link between macropore 3-D characteristics and measured flow and transport properties. The general set up of our experiment is shown in Fig. 2. A PVC cap was placed at the top of each soil column, with high vacuum grease (Dow Corning Corp., Midland, MI) used to prevent air leakage between the PVC pipe and the cap. A flow distributor was placed at the column bottom using a pipe fitting and clamp. The procedure of vacuum saturation described by Flint and Flint (2002) was followed. First, the vessel was placed under a vacuum for about 30 min at a pressure of 34 kPa. While maintaining this vacuum, a 0.005 M CaSO$_4$ solution slowly entered the soil column from the bottom at a rate of 6 mL min^{-1}. A piece of filter paper (Grade 417; VWR International, West Chester, PA) was placed at the bottom of the soil column to protect the soil when water moved into the column (this filter paper also prevented clay colloids from clogging the outlet during the breakthrough experiments). When solution was observed in the clear tube at the top of the PVC cap, water flow was stopped and the soil was left under vacuum for about 3 d for the soil to equilibrate with the solution. Before and after saturation, the weight

of the soil column and all the accessories was determined to estimate initial soil water content and saturated ratio.

After saturation, K_{sat} of the whole soil column and each horizon within the column, as well as the breakthrough curve (BTC) were determined (Fig. 2b). Pressure transducers (OMEGA Engineering, INC., Stamford, CT) were used to measure the pressure differences between each horizon boundaries. A constant hydraulic head was maintained with a Mariotte siphon. The flow rate was adjusted by changing the hydraulic head (ΔH), that is, the height of the outlet tube (Fig. 2b). At a constant hydraulic head, when the readings of all the pressure transducers were constant, the flow rate was measured and the pressure differences were recorded. The flow rate was plotted against the pressure difference and K_{sat} was determined from the slope according to Darcy's Law. At least four different flow rates were used to obtain reliable results for each soil horizon contained within each column as well as for the whole column.
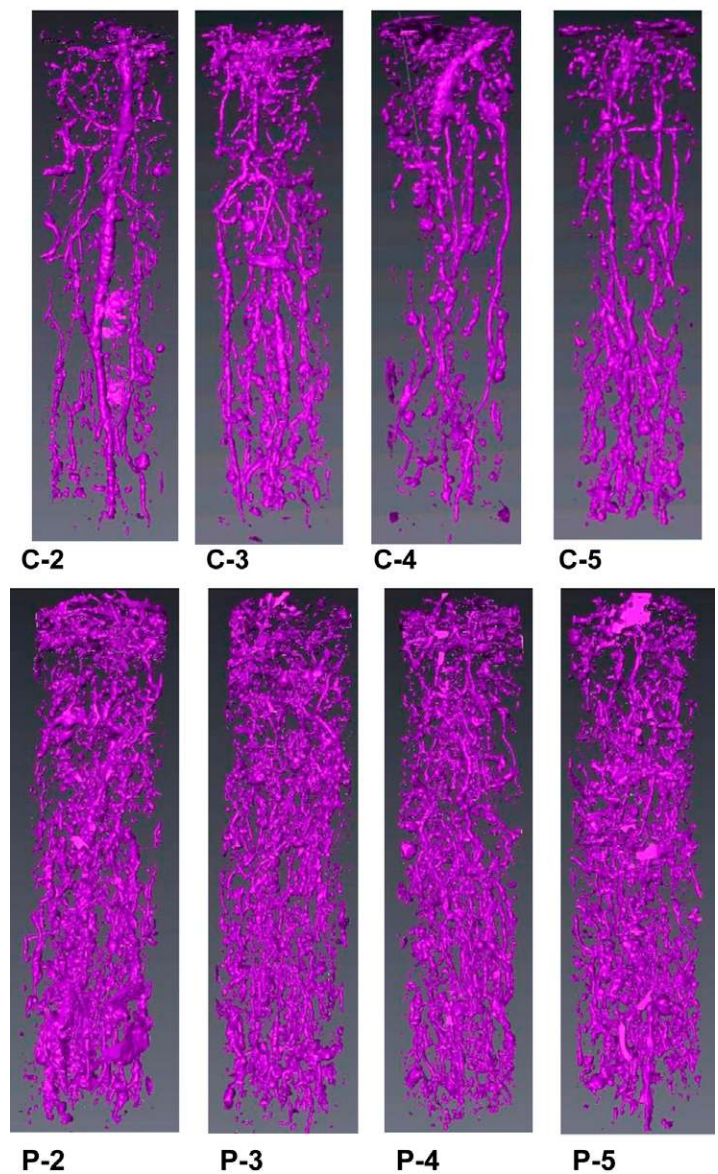

Fig. 1. Three-dimensional visualization of soil macropore networks in the eight soil columns studied. Each column is 102 mm in diameter and about 350 mm in vertical length. The label C stands for cropped land and P stands for pastured land. The number after C or P is replicated column number.

Table 2. Quantified macropore characteristics and their definitions used in this study.

Characteristics	Definition
Macroporosity, $m^3\ m^{-3}$	The fraction of macropore volume over total soil volume considered.
Length density, $km\ m^{-3}$	The total length of macropores in a unit volume of soil.
Node density, number m^{-3}	The number of nodes in a unit volume of soil. A node is defined as an intersection where two pore branches are connected, which can be used to quantify the inter-connectivity of macropores.
Macropore network density, number m^{-3}	The number of macropore networks (isolated macropore or a group of interconnected macropores) in a unit volume of soil.
Path number, number	The number of independent and continuous macropore paths between two boundaries. For example, when path number is equal to 2 for a soil horizon, it means there are two independent and continuous paths of macropores that run through the entire horizon.
Mean tortuosity	The ratio of total actual macropore length to total straight line distance of all macropores in a certain volume of soil.
Mean hydraulic radius, cm	Calculated from the total volume and total actual length of macropores by assuming that macropores are cylindrical.
Angle, °	The angle away from vertical to characterize the inclination of a macropore.
Length$_{150}$, cm	The total vertical length of macropores with vertical length >150 mm.
Tortuosity$_{150}$	The mean tortuosity of macropores with vertical length >150 mm.
Angle$_{150}$, °	The mean angle of macropores with vertical length >150 mm.

By observing the pressure difference between the soil horizons and the whole soil column (Fig. 2b), we noticed that the filter paper contributed to some pressure drop. Such effect from the filter paper at the bottom of the soil column was most evident in one of the eight columns (i.e., C-2 in Table 3) where an earthworm channel passed through that entire column. In addition, clay colloids that might have migrated down during the flow experiment could have possibly clogged some pore space of the filter paper, resulting in decreased filter paper conductivity (Hillel, 1998, p. 183–189). Because of this concern, we decided to use the calculated harmonic mean of the soil column K_{sat} (i.e., horizon-thickness-weighted mean K_{sat} based on each horizon's measured K_{sat}) to represent the overall effective K_{sat} of each column in the subsequent analysis (Hillel, 1998, p. 183–189; Jury and Horton, 2004):

$$K_{sat\ column} = \frac{L_T}{\dfrac{L_{h1}}{K_{sat\ h1}} + \dfrac{L_{h2}}{K_{sat\ h2}} + \dfrac{L_{h3}}{K_{sat\ h3}}}, \qquad [1]$$

where $K_{sat\ column}$, $K_{sat\ h1}$, $K_{sat\ h2}$, and $K_{sat\ h3}$ are K_{sat} of the whole column and horizons of Ap1, Ap2, and Bt1, respectively; L_T, L_{h1}, L_{h2}, and L_{h3} are the length of the whole column and the three soil horizons, respectively. The resulting calculated K_{sat} is 1.11 to 4.87 times larger than the measured whole column K_{sat} (Table 3).

Calcium bromide BTCs were determined at a flow rate of about 10 mL min^{-1} for all the eight soil columns. When the flow rate was constant, a 0.005 M CaBr$_2$ solution was quickly used to replace the 0.005 M CaSO$_4$ solution. Meanwhile, the effluent was collected with an automatic fractional collector CF-1 Fraction Collector (Spectrum Chromatography Inc., Houston, TX) at intervals of 2 min during the first 3 h and 10 min afterward. About 7 mL of solution was obtained for each sample. The Br concentration was then determined for each solution sample by flow injection analysis using a Lachat autoanalyzer (Quick Chem FIA+ 8000 Series, Lachat Instruments, Loveland, CO) following the method described by Bogren and Smith (2003).
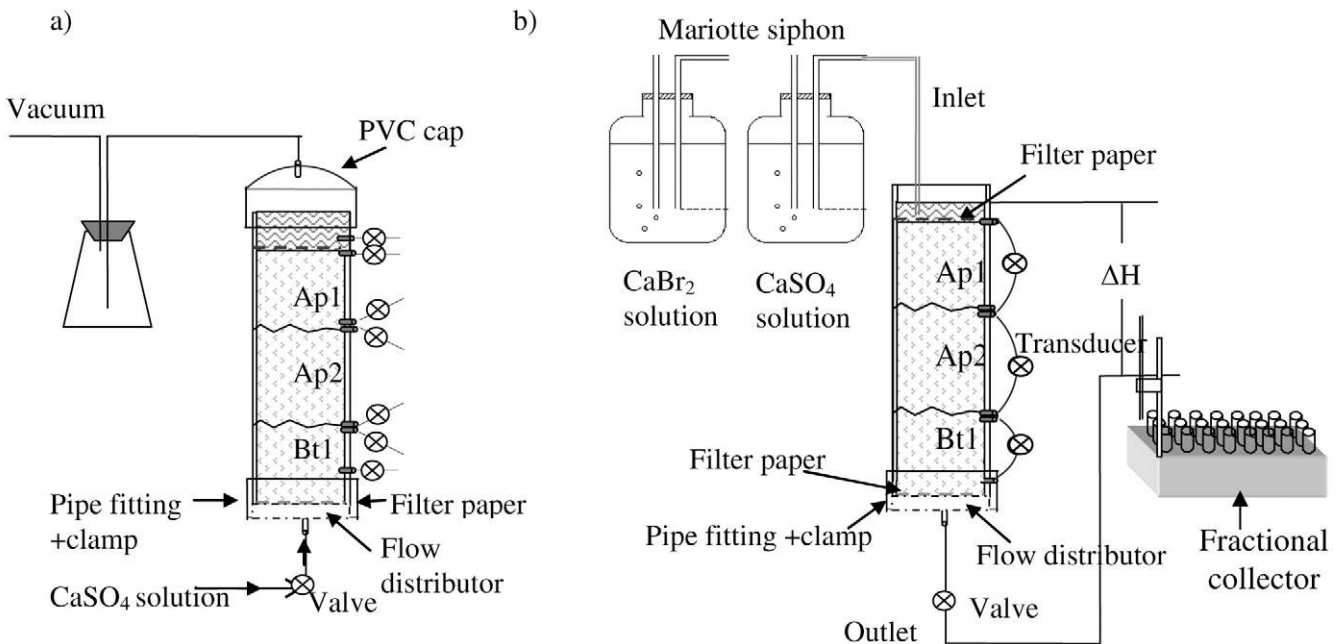

Fig. 2. Experimental setup used in this study to (a) saturate the soil column using a vacuum and (b) determine saturated hydraulic conductivity of the whole column as well as individual soil horizons and solute (CaBr$_2$) breakthrough curve.

Table 3. Saturated hydraulic conductivity (K_{sat}) determined for the whole soil columns and individual soil horizons within each column. The number in the parentheses of the last column is the standard error. Cropped soil is labeled as C and pastured soil is labeled as P. The number after C or P is replicate number. The calculated whole column K_{sat} is the harmonic mean of the measured K_{sat} of the three horizons contained within each column (see the text for explanation).

Soil column or horizon	C-2	C-3	C-4	C-5	Geometric mean	P-2	P-3	P-4	P-5	Geometric mean
					cm min^{-1}					
Ap1 horizon	43.37	0.29	1.39	0.36	1.65 (3.71)	2.11	7.18	1.75	1.30	1.69 (1.05)
Ap2 horizon	30.13	0.47	0.41	0.64	2.09 (3.11)	10.27	5.27	1.20	1.33	2.54 (1.27)
Bt1 horizon	1.68	0.25	-†-	1.37	0.83 (1.36)	0.62	1.36	0.42	0.06	0.25 (1.72)
Whole column (measured)	2.11	0.23	0.21	0.42	0.59 (0.60)	1.30	1.05	0.78	0.09	0.46 (0.26)
Whole column (calculated)	10.26	0.26	-†-	0.51	1.11 (1.47)	2.29	4.56	1.19	0.40	1.03 (1.45)

†Data missing.

Breakthrough Modeling

Chemical BTCs were quantitatively evaluated using the computer program CXTFIT (Toride et al., 1995). Both a traditional convection–dispersion model (i.e., equilibrium model) and a two-region model (i.e., nonequilibrium model) in CXTFIT were used to inversely estimate flow and transport parameters. The equilibrium model is written as:

$$\frac{\partial(\theta C)}{\partial t} = \frac{\partial}{\partial x}\left(\theta D \frac{\partial C}{\partial x} - j_w C\right) , \qquad [2]$$

where θ is volumetric soil water content (m^3 m^{-3}), t is time (min), C is solute concentration (g mL^{-1}), x is the vertical coordinate (cm), D is solute dispersion coefficient (cm^2 min^{-1}), and j_w is water flux (cm min^{-1}). Assuming negligible diffusion, dispersivity, λ (cm), is given by:

$$\lambda = D/v , \qquad [3]$$

where v is mean pore-water velocity in the soil column (cm min^{-1}). The non-equilibrium model is described as (Toride et al., 1995):

$$\theta_m \frac{\partial C_m}{\partial t} = \theta_m D_m \frac{\partial^2 C_m}{\partial x^2} - j_w \frac{\partial C_m}{\partial x} - a(C_m - C_{im}) , \qquad [4]$$

where θ_m, C_m, and D_m are volumetric water content (m^3 m^{-3}), solute concentration (g mL^{-1}), and dispersion coefficient (cm^2 min^{-1}) of the mobile domain, respectively; a is the first-order mass transfer coefficient (min^{-1}), and C_{im} (g mL^{-1}) is the solute concentration of the immobile domain. The unknown model parameters were estimated using a nonlinear least-square optimization approach based on the Levenberg–Marquardt method (Toride et al., 1995). For the traditional convection–dispersion equation, the dispersion coefficient was inversely estimated by fitting the BTC. For the two-region model, the fraction of mobile water content to total water content (θ_m/θ), the coefficient of lateral mass exchange (a), and the dispersion coefficient (D_m) of the mobile domain were inversely estimated based on the measured BTC.

Statistical Analysis

Stepwise regression was used to correlate the macropore characteristics (determined from the 3-D macropore networks) to the K_{sat} and solute dispersion coefficient using Minitab (Minitab Inc, State College, PA). The option of standard stepwise regression combining the backward and forward selection was selected. The α was set to 0.15 to enter and remove a variable. The comparison of slopes of linear regression was performed within the REG procedure of SAS (SAS Institute Inc., Cary, NC).

RESULTS AND DISCUSSION
Saturated Hydraulic Conductivity and its Relationship to Macropore Characteristics

Saturated hydraulic conductivity of the soils studied was a function of both total macroporosity and macropore geometry. Despite considerable variability within each of the two land uses, there was greater macroporosity lower bulk density, higher organic matter content, and more developed structure, in the pasture soil horizons (mainly A1 and A2 horizons) (Fig. 1), leading to generally higher K_{sat} than that in the cropland soils (Table 1). The only exception to this observation was the C-2 cropland column, where an earthworm burrow was observed through the entire column, providing a much greater K_{sat} (43.37, 30.13, and 1.68 cm min^{-1} for the Ap1, Ap2, and Bt1 horizons, respectively) than that observed in the other cropland columns (Table 3). The K_{sat} for the whole C-2 column was one order of magnitude higher than those for the other cropland columns. This indicated that the single earthworm burrow contributed dominantly to the high K_{sat} value in the C-2 column. Bastardie et al. (2003) also reported exceptionally high K_{sat} for soil columns containing earthworm burrows (up to 264 cm min^{-1}). Cey and Rudolph (2009) showed that film and rivulet flow along macropores yielded vertical flow velocity exceeding 2.8 cm min^{-1}. Saturated hydraulic conductivity was highly variable, even within the same land use (Table 3), and previous studies have shown that K_{sat} in field soils is often highly variable and its statistical distribution is generally highly skewed because of spatial variation in soil pore features, especially macropore characteristics (Warrick and Nielsen, 1980). Therefore, the natural logarithm of K_{sat} value was used in the regression analyses.

The difference in the regression slope for the natural logarithm of K_{sat} value against macroporosity between the two land uses (i.e., 54.0 for cropland and 37.7 for pasture) ($p < 0.1$) (Fig. 3) reflects the impacts from different macropore geometrical features. Compared with the pasture soil, the macropores in the cropland soil were less tortuous, more vertically oriented and more continuous (Fig. 1); consequently, K_{sat} increased more quickly with an increase in unit macroporosity for cropland as compared with pasture. The mean tortuosity for cropland was 1.58, 1.47, and 1.47 for the Ap1, Ap2, and Bt horizons, respectively, while the mean tortuosity for pasture was 1.83, 1.69, and 1.62 for the Ap1, Ap2, and Bt horizons, respectively. In addition, the cropland soil had a higher proportion of highly
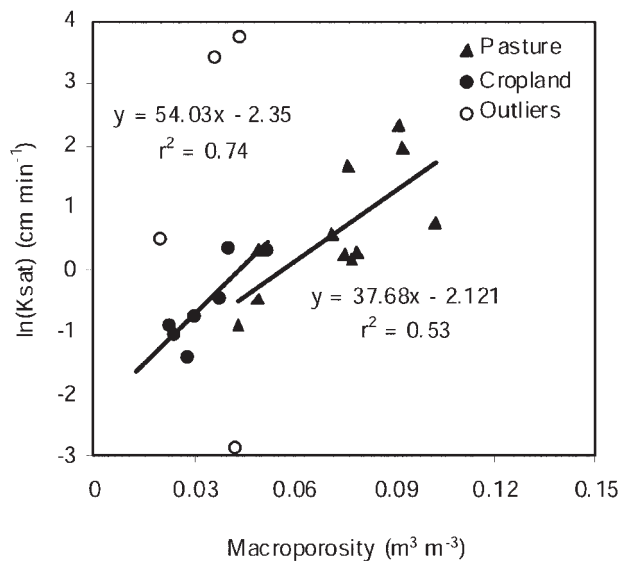
Fig. 3. The relationship between K_{sat} and macroporosity of each soil horizon in the eight soil columns from the two land uses (cropland and pasture). The K_{sat} of the three horizons in column C-2 of the cropped land (i.e., the three open circles in this diagram above the regression line) and the Bt1 horizon of P-5 (the open circle in this diagram below the regression line) were considered outliers because of the earthworm channel passing through the entire C-2 column or the Bt1 horizon of the P-5 column.

continuous macropores (>45 mm) than those of the pasture soil (Luo et al., 2010). Because of the less tortuous, more vertically oriented, and continuous macropores in the cropland soil, the macropores there were more effective in conducting water than those in the pasture counterpart (Fig. 3) and would also likely lead to a higher degree of preferential flow.

For all eight soil columns, the K_{sat} of each horizon was well predicted by macroporosity plus path number (the number of macropores passing through a given volume, either for an entire soil column or a horizon) ($R^2 = 0.71$; Fig. 4a), while 78% of the variability in K_{sat} of the whole soil column could be explained by path number and length density ($R^2 = 0.78$). However, macroporosity and path number also predicted well the K_{sat} of the whole soil column ($R^2 = 0.75$; Fig. 4b), implying that macroporosity and macropore length density (the total length of macropores in a unit volume) represented similar hydraulic characteristics in these soils. Instead of determining length density, soil macroporosity can be more easily determined using indirect methods such as a water retention curve (Ersahin et al., 2002), a tension infiltrometer (Zhou et al., 2008), or by a direct method such as imaging used in this study. The path number can be considered as an indicator of highly continuous macropores. Previous investigations have illustrated the importance of macropore continuity to water flow through soils (Smettem, 1986; Bastardie et al., 2003).

Compared with macropore characteristics, basic soil properties such as those listed in Table 1 could not be used to predict soil horizon K_{sat} values as well as macropore characteristics. Clay content and bulk density displayed negative relationships with the soil horizon K_{sat} values, with each explaining 52.6 and

$$\ln(Ksat) = -2.61 + 3.63* \text{path number} + 46.7* \text{macroporosity}$$

$$\ln(Ksat) = -2.186 + 3.277* \text{path number} + 33.90* \text{macroporosity}$$
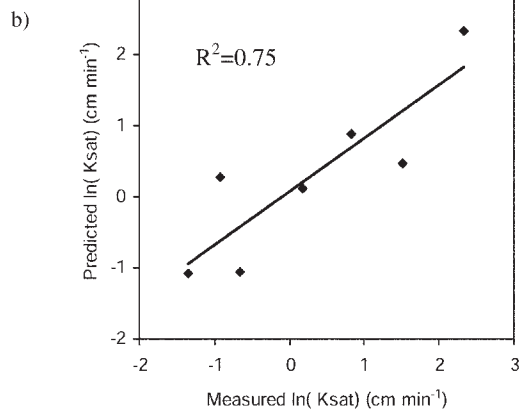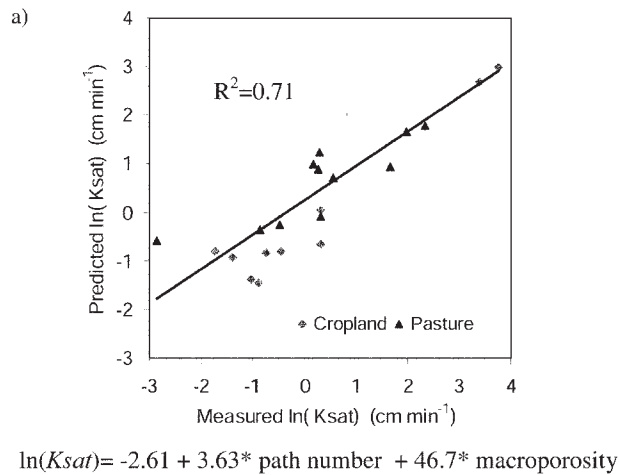
Fig. 4. Relationships between macropore characteristics and K_{sat} for (a) each soil horizon contained in the eight soil columns (note the Bt1 horizon data for the C-4 column was missing) and (b) the whole soil columns (note the C-4 column was not included because of its missing Bt1 horizon data). The predicted K_{sat} was determined from macropore characteristics using the equation indicated under each figure. The R^2 was determined from the linear regression of predicted vs. observed K_{sat} values.

26.5% of the variability in the geometric mean values of the individual horizon K_{sat}, respectively. Organic matter content, silt content, and sand content correlated positively with soil horizon K_{sat}, but each explained 21.0, 10.9, and 6.7% of the variability in the K_{sat} geometric mean values, respectively.

Solute Transport and its Relationship to Macropore Characteristics

All the BTCs showed a quick response and a long tail, clearly indicating the occurrence of preferential flow (Fig. 5). At one pore volume, the mean relative concentration of the effluent was 79.1% of the original input for the cropland and 70.0% for the pasture. Except for column C-2, the equilibrium CDE fitted the BTCs well for all the soil columns ($r^2 > 0.97$) (Fig. 5). This implies that the dispersion coefficient performed well in simulating the effluent solute flux in these soil columns, ones with a considerable amount of biopores. But for Column C-2, the non-equilibrium model improved the simulated fit to the actual effluent BTC (Fig. 6), r^2 increased from 0.91 to 0.99.

The resultant fraction of mobile water content to total water content was 0.07, the dispersion coefficient in the macropore domain was 78.9 $cm^2 min^{-1}$, and the coefficient of lateral mass exchange was 0.00015 min^{-1}. These values indicate a high degree of preferential flow and a low degree of interaction between the mobile and immobile domains in column C-2.

Although the pasture soil generally had greater macroporosity compared with the cropland soil (0.028 $m^3 m^{-3}$ for the cropland and 0.061 $m^3 m^{-3}$ for the pasture; Fig. 1), the solute breakthrough was generally faster in the cropland than in the pasture (Fig. 5). The greater amount of macropores in the pasture soil was more evenly distributed and the macropores were not as straight and vertically continuous as those observed in the cropland soil (Fig. 1). Additionally, the pasture soil had better developed smaller aggregates (i.e., strong fine to medium granular aggregates) than that in the cropland soil (moderate fine to medium subangular aggregates) (Table 1). Thus, flow and transport would occur more uniformly in the pasture soil than in the cropland soil, leading to higher λ values in the latter.

Besides comparing the breakthrough of solute (i.e., relative flux concentration at certain pore volume), we can also use the values of λ to compare the degree of preferential flow between the two land uses. The greater the λ value corresponds to increasing degree of preferential flow (Vervoort et al., 1999). The λ value estimated from the equilibrium model was 43.72 cm for C-2 and 3.80 cm for C-5 (Fig. 5). These high values were due to the presence of highly continuous and vertically oriented macropores in these two soil columns. The other two cropland soil columns had λ values of 1.16–1.17 cm. In comparison, the λ values for the pasture soil columns ranged from 0.75 to 1.59 cm, with an average of 1.17 cm (Fig. 5). Similar to the K_{sat} results, the λ values in the soil columns studied were highly variable because of considerable macropore spatial variability. This suggests that the sample volume in this study might still be less than the representative elementary volume needed for the K_{sat} and λ measurements in these highly macroporous soils, and thus larger sample volumes or a greater number of samples would be needed to obtain statistically more stable results.

The path number, hydraulic radius, and angle$_{150}$ (the mean angle for macropores longer than 150 mm) best explained the variability in the inversely estimated natural logarithm of λ values ($R^2 = 0.97$) (Fig. 7). According to this relationship, the dispersion
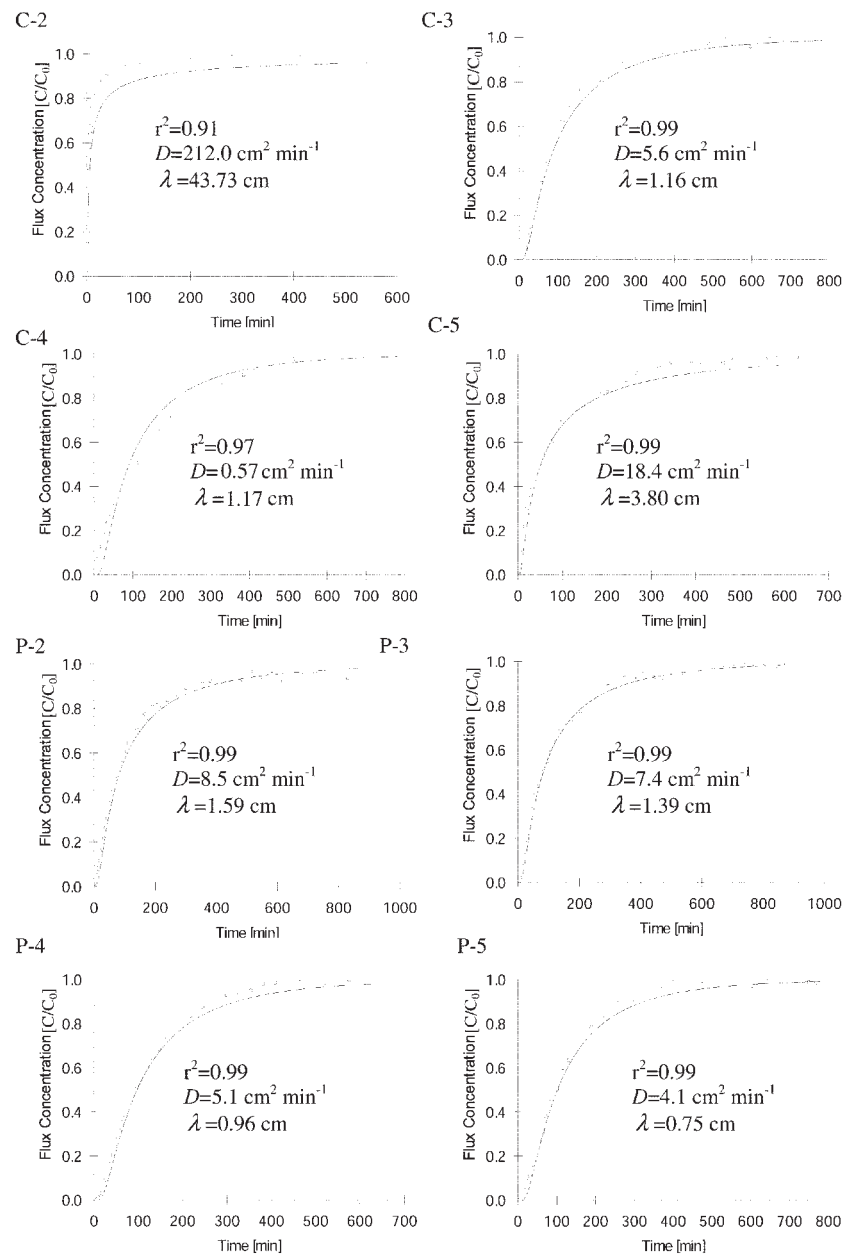

Fig. 5. Measured (dots) and fitted (line) breakthrough curves using an equilibrium convection-dispersion equation (CDE) for each of the eight soil columns. The dispersion coefficient (D) was inversely estimated in each column. The dispersivity (λ) was calculated from D, flow rate (i.e., 10 cm min^{-1}), and porosity. The label C stands for cropped land and P stands for pastured land. The number after C or P is replicated column number.

within the soil column was mainly influenced by macropore size (hydraulic radius), connectivity (path number), and inclination (angle$_{150}$). The high λ in column C-2 can be mostly attributed to path number (path number = 1). Hydrodynamic dispersion increases with an increase in macropore hydraulic radius, and the degree of vertical inclination of highly continuous macropores also positively impacts the chemical dispersion along the flow direction. It is interesting to note that the λ values for the whole soil columns were most closely related to the K_{sat} of the Bt horizons ($r^2 = 0.79$) rather than the K_{sat} of the whole soil columns, Ap2, or Ap1 horizons (Fig. 8). This implies that the dispersivity may be mainly controlled by the layer with the lowest conductivity, that is, the Bt horizon in this study, which had a

$$\ln(\lambda) = -7.548 + 2.83* \text{path number} + 12*\text{hydraulic radius} - 0.072*\text{angle}_{150}$$
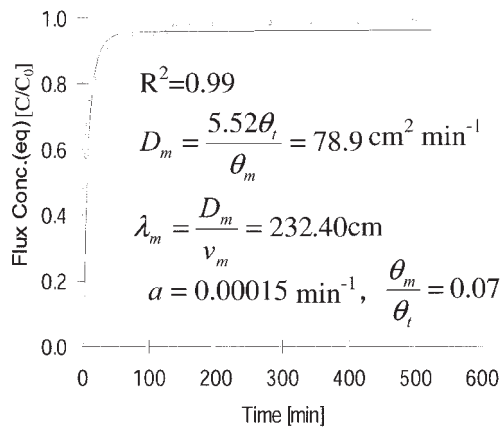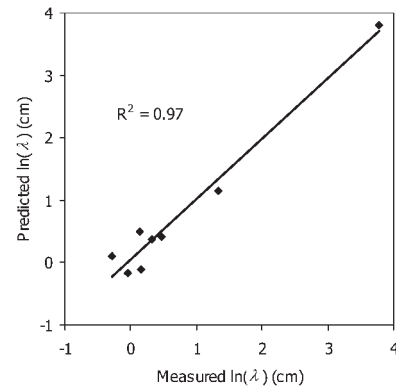
Fig. 6. Measured (dots) and fitted (line) breakthrough curve using a non-equilibrium two-region model for the Column 2 of the cropped land (C-2). The fraction of mobile water content to total water content (θ_m/θ), the coefficient of lateral mass exchange (a), and the dispersion coefficient (D_m) of the mobile domain were inversely estimated. The mobile domain dispersivity (λ_m) was calculated from D_m and fraction of the mobile domain.

Fig. 7. Relationship between macropore characteristics and dispersivity (λ) in the eight soil columns studied. The predicted λ was obtained using the equation indicated under the figure. The R^2 was determined from the linear regression of predicted vs. observed natural logarithm of λ values. Angle$_{150}$ is the mean angle for macropores longer than 150 mm. Note the highest point in the graph was from the column C-2 with a single earthworm hole passing through the entire column. The λ of the C-2 column was obtained using the equilibrium model.

higher clay content, a higher bulk density, a lower organic matter content, and a lower degree of structural development compared with the A horizons (Table 1).

SUMMARY AND CONCLUSIONS

This study investigated quantitative relationships between macropore characteristics and two major flow and transport parameters (i.e., K_{sat} and λ) for eight intact soil columns from two land uses. Macropores played an important role in saturated water flow and solute transport in all cases, which was a dominant

control of soil K_{sat}, with macroporosity and path number being the best predictors of K_{sat} values. In our study, soil macroporosity also correlated closely with macropore surface area, network density, length density, and node density despite differences in soil types and land uses (Luo et al., 2010). Path number (the number of macropores that pass through a given volume, either an entire soil column or a soil horizon) was critical to flow and transport when highly continuous macropores were present.

The equilibrium CDE model described well the BTCs of the soil columns studied when there was no continuous macropore throughout the entire column. Although with lower total amount of macropores than the pasture soils, the cropland soils displayed a greater degree of preferential flow in terms of their heterogeneous flow distribution and the related higher λ values. The path number, hydraulic radius, and macropore angle best explained the variability in the observed natural logarithm of λ values ($R^2 = 0.97$). Additionally, the overall λ values of the whole soil columns appeared to be mainly controlled by the soil layer with the lowest K_{sat}.

Our results indicate that the best predictors of saturated soil hydraulic parameters include macroporosity, path number, hydraulic radius, and macropore angle. Due to the time-consuming nature of this study, only one soil type was investigated. Therefore, cautions should be exercised when using the regression
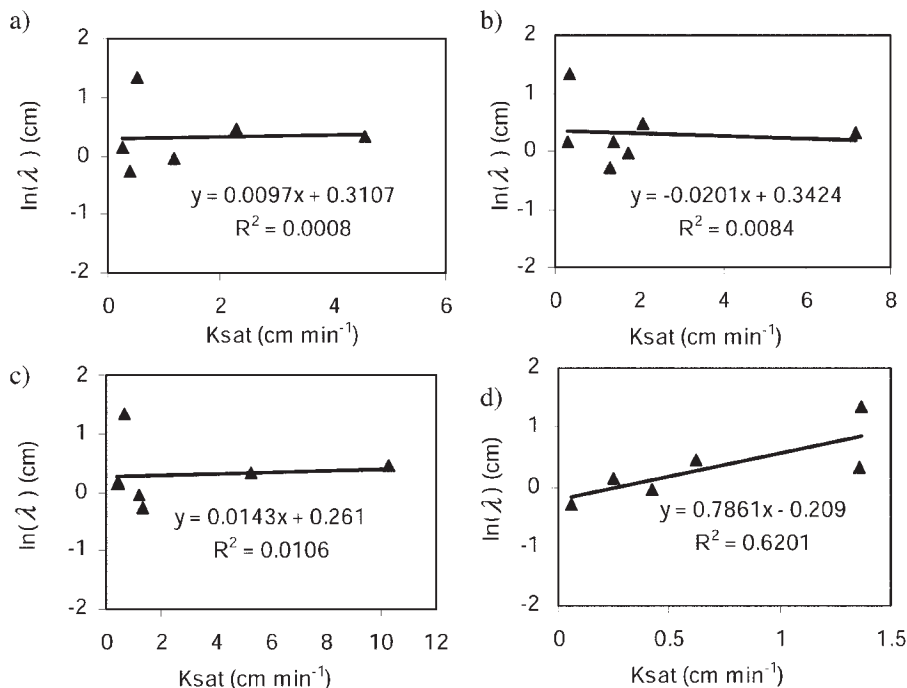

Fig. 8. Relationships between dispersivity (λ) and saturated hydraulic conductivity (K_{sat}) in the soil columns studied for (a) the whole soil columns, (b) the Ap1 horizons, (c) the Ap2 horizons, and (d) the Bt1 horizons. Data from the column C-2 was not included here because of the extremely high values in K_{sat} and λ caused by a single earthworm hole that passed through the entire column. Also there was a missing data point for the Bt1 horizon of the C-4 column.

results obtained from this study. As the non-invasive imaging techniques such as X-ray CT become more widely available, quantitative data of soil structural features, especially 3-D macropore networks, would become more readily obtainable. We therefore encourage more efforts to continuously test and quantify the overall relationships between soil macropore characteristics and flow and transport parameters in a broad range of soil types, land uses, and management practices. Also note that this study was conducted under saturated condition, thus studies on unsaturated flow are needed to further investigate the hydraulic effectiveness of macropores and their influences on water movement and chemical transport under varying degrees of saturation.

ACKNOWLEDGMENTS

REFERENCES

Anderson, S.H., R.L. Peyton, J.W. Wigger, and C.J. Gantzer. 1992. Influence of aggregate size on solute transport as measured using computed-tomography. Geoderma 53:387–398.

Anderson, S.H., H. Wang, R.L. Peyton, and C.J. Gantzer. 2003. Estimation of porosity and hydraulic conductivity from x-ray CT-measured solute breakthrough. p. 135–150. *In* F. Mees et al. (ed.) Applications of x-ray computed tomography in the geosciences. Spec. Publ. 215. Geol. Soc., London.

Akay, O., and G.A. Fox. 2007. Experimental investigation of direct interconnectivity between macropores and subsurface drains during infiltration. Soil Sci. Soc. Am. J. 71:1600–1606.

Arya, L.M., and J.F. Paris. 1981. A physicoempirical model to predict soil moisture characteristic from particle-size distribution and bulk density data. Soil Sci. Soc. Am. J. 45:1023–1030.

Bastardie, F., Y. Capowiez, J.-R. Dreuzy, and D. Cluzeau. 2003. X-ray tomographic and hydraulic characterization of burrowing by three earthworm species in repacked soil cores. Appl. Soil Ecol. 24:3–16.

Beven, K., and P. Germann. 1982. Macropores and water flow in soils. Water Resour. Res. 18:1311–1325.

Bogren, K., and P. Smith. 2003. Determination of Bromide by flow injection analysis: QuickChem Method 10–135–21–2-B FIA Methodology. Lachat Instruments, Loveland, CO.

Bouche, M.B., and F. Al-Addan. 1997. Earthworms, water infiltration, and soil stability: Some new assessments. Soil Biol. Biochem. 29:441–452.

Cey, E.E., and D.L. Rudolph. 2009. Field study of macropore flow processes using tension infiltration of a dye tracer in partially saturated soils. Hydrol. Processes 23:1768–1779.

Ersahin, S., R.I. Papendick, J.L. Smith, C.K. Keller, and V.S. Manoranjan. 2002. Macropore transport of bromide as influenced by soil structure differences. Geoderma 108:207–223.

Flint, A.L., and L.E. Flint. 2002. Particle density. p. 233–234. *In* J.H. Dane, and G.C. Topp, (ed.) Methods of soil analysis. Part 4. SSSA Book Series No. 5. SSSA, Madison, WI.

Franklin, D.H., L.T. West, D.E. Radcliffe and P.F. Hendrix. 2007. Characteristics and genesis of preferential flow paths in a Piedmont Ultisol. Soil Sci. Soc. Am. J. 71:752–758.

Goncalves, M.C., F.J. Leij, and M.G. Schaap. 2001. Pedotransfer functions for solute transport parameters of Portuguese soils. Eur. J. Soil Sci. 52:563–574.

Hillel, D. 1998. Environmental soil physics. Academic Press. San Diego, CA.

Jarvis, N.J. 2007. A review of non-equilibrium water flow and solute transport in soil macropores: Principles, controlling factors and consequences for water quality. Eur. J. Soil Sci. 58:523–546.

Jury, W., and R. Horton. 2004. Soil Physics. 6th ed. Wiley, Hoboken, NJ.

Kettler, T.A., J.W. Doran, and T.L. Gilbert. 2001. Simplified method for soil particle-size determination to accompany soil-quality analyses. Soil Sci. Soc. Am. J. 65:849–852.

Kosugi, K. 1999. General model for unsaturated hydraulic conductivity for soils with lognormal pore-size distribution. Soil Sci. Soc. Am. J. 63:270–277.

Köhne, J.M., and B.P. Mohanty. 2005. Water flow processes in a soil column with a cylindrical macropore: Experiment and hierarchical modeling. Water Resour. Res. 41:W03010 10.1029/2004WR003303.

Lin, H.S., K.J. McInnes, L.P. Wilding, and C.T. Hallmark. 1996. Effective porosity and flow rate with infiltration at low tensions into a well-structured subsoil. Trans. ASAE 39:131–135.

Lin, H.S., K.J. McInnes, L.P. Wilding, and C.T. Hallmark. 1999. Effects of soil morphology on hydraulic properties: II. Hydraulic pedotransfer functions. Soil Sci. Soc. Am. J. 63:955–961.

Luo, L.F., H.S. Lin, and P. Halleck. 2008. Quantifying soil structure and preferential flow in intact soil using X-ray computed tomography. Soil Sci. Soc. Am. J. 72:1058–1069.

Luo, L.F., H.S. Lin, and S.C. Li. 2010. Quantification of 3-D soil macropore networks in different soil types and land uses using computed tomography. J. Hydrol. (in press).

Luxmoore, R.J., P.M. Jardine, G.V. Wilson, J.R. Jones, and L.W. Zelszny. 1990. Physical and chemical controls of preferred path flow through a forested hillslope. Geoderma 46:139–154.

Mallants, D., P.H. Tseng, N. Toride, A. Timmerman, and J. Feyen. 1997. Evaluation of multimodal hydraulic functions in characterizing a heterogeneous field soil. J. Hydrol. 195:172–199.

Merdun, H., and V.L. Quisenberry. 2004. Relating model parameters to basic soil properties. Aust. J. Soil Res. 42:841–849.

Pachepsky, Y., and W.J. Rawls. 2004. Development of pedotransfer functions in soil hydrology. Elsevier, Amsterdam, and the Netherlands.

Perret, J., S.O. Prasher, A. Kantzas, and C. Langford. 2000. A two-domain approach using CAT scanning to model solute transport in soil. J. Environ. Qual. 29:995–1010.

Schaap, M.G., and I. Lebron. 2001. Using microscope observations of thin sections to estimate soil permeability with the Kozeny-Carman equation. J. Hydrol. 251:186–201.

Schulte, E.E., and B.G. Hopkins. 1996. Estimation of soil organic matter by weight loss on ignition. p. 21–31. *In* F.R. Magdoff et al. (ed.) Soil organic matter: Analysis and interpretation. SSSA Spec. Publ. 46. SSSA, Madison, WI.

Shaw, J.N., L.T. West, D.E. Radcliffe, and D.D. Bosch. 2000. Preferential flow and pedotransfer functions for transport properties in sandy Kandiudults. Soil Sci. Soc. Am. J. 64:670–678.

Smettem, K.R.J. 1986. Analysis of water flow from cylindrical macropores. Soil Sci. Soc. Am. J. 50:1139–1142.

Toride, N., F.J. Leij, and M.Th. van Genuchten. 1995. The CXTFIT code for estimating transport parameters from laboratory or field tracer experiments. Version 2.0. Res. Rep. 137. U.S. Salinity Lab. Agric. Res. Service, U.S. Dep. of Agric., Riverside, CA.

van Genuchten, M.Th. 1980. A closed-form equation for predicting the hydraulic conductivity of unsaturated soils. Soil Sci. Soc. Am. J. 44:892–898.

Vervoort, R.W., D.E. Radcliffe, and L.T. West. 1999. Soil structural development and preferential solute flow. Water Resour. Res. 35:913–928.

Vervoort, R.W., and S.R. Cattle. 2003. Linking hydraulic conductivity and tortuosity parameters to pore space geometry and pore-size distribution. J. Hydrol. 272:36–49.

Warrick, A.W., and D.R. Nielsen. 1980. Spatial variability of soil properties in the field. p. 319–344. *In* D. Hillel (ed.) Applications of soil physics. Academic Press, New York.

Zhou, X., H.S. Lin, and E.A. White. 2008. Surface soil hydraulic properties in four soil series under different land uses and their temporal changes. Catena 73:180–188.